A Design Investigation of A 1 MVA SiC Medium Voltage Three Phase Rectifier Based on Isolated Dual Active Bridge

Hanning Tang, *Member, IEEE*, Alex Q. Huang, *Fellow, IEEE*

The University of Texas at Austin, TX 78712, USA
{hanningtang, aqhuang}@utexas.edu

***Abstract*— Dual-active-bridge (DAB) isolated three phase power factor correction (PFC) rectifier is attracting more and more attentions from academia and industry because of high power density, operational flexibility and premium performance, etc. This paper gives an overview to adapt the DAB PFC rectifier to medium voltage (MV) variable frequency drive (VFD) applications. First, a novel medium voltage drive (MVD) topology and its operating conditions are illustrated. Second, as the core component used in the DAB rectifier, a hypothetic silicon carbide (SiC) metal oxide semiconductor field effect transistor (MOSFET) module rated at 12.5 kV, 375 A is proposed. The electrical, namely power loss, and thermal models are developed. Third, the control scheme of the grid-tied DAB rectifier is investigated. Analysis and simulations have been carried out to verify the proposal.**

***Index Terms*—Dual Active Bridge (DAB), Isolated Three Phase Power Factor Correction (PFC) Rectifier, Variable Frequency Drive (VFD), Silicon Carbide (SiC), Metal Oxide Semiconductor Field Effect Transistor (MOSFET).**

I. INTRODUCTION

Modern power electronics have revolutionized the path of medium voltage motor drive (MVD) industry by introducing the variable frequency drive (VFD) technology (also known as Adjustable Speed Drive (ASD) or Frequency Converters (FC)). Medium voltage (MV) VFD products have been widely deployed in eight major industrial applications, including mining/cement, petrochemical, metals, paper/pulp, marine, oil/gas, power generation and water/waste water. A MVD improves energy efficiency and meets the end users' requirements by controlling the motor at an optimal speed and torque [1] [2]. In the meanwhile, it monitors and manipulates the utility power grid interface to compensate the negative influences introduced by the machine. One of the major concerns is to mitigate the harmonics caused by the MVDs which deteriorate the grid power quality. Besides, the customers challenge the manufacturing industry to design next generation MVDs with more technical, operational and economic feasibilities.

A modern three level neutral point clamped inverter (3L NPC), equipped with phase-shifting transformers, is presented in Fig. 1. With no active front-end (AFD) requirement, a diode based rectifier is back-to-back connected to the 3L NPC inverter. A twenty-four pulse transformer rectifier improves grid side power quality to meet IEEE Std 519 harmonic control requirements. The DC buffer provides a smooth power to the rear-end inverter. Thereby, the rear-end inverter is decoupled from the front-end rectifier from both electrical connection and system control loops. Output dv/dt or sinusoid filter is optional to protect motor windings from over voltage caused by long motor cables and pulse width modulation (PWM) inverter control schemes [3].

A AC-DC rectifier, being placed at the front side of the MVD systems, addresses the current distortion issue and guarantees the system stability and reliability [4]. Power factor correction (PFC) feature is attractive in numerous business cases since it reduces the system operating costs in the long term.

A 12-pulse, 18-pulse or 24-pulse rectifier based on phase-shifting transformers is advocated by MVD manufactures because it provides the galvanic isolation capability and serves as additional failure buffer if either inverter or motor is under abnormal circumstances. A 12-pulse rectifier obtains a Total Harmonic Distortion (THD) in the range of 10 % to 15 %. The THD value decreases with higher pulse rectifier. However, it impairs the power density and limits the product adaption in some space limited applications, such as electric locomotive and high speed rail. Another disadvantage which prevents traditional MVDs from entering in the renewable energy market is the lack of the operational feasibility; e.g. the input current THD and power factor will be further deteriorated when the motor is partially loaded [2] [5].

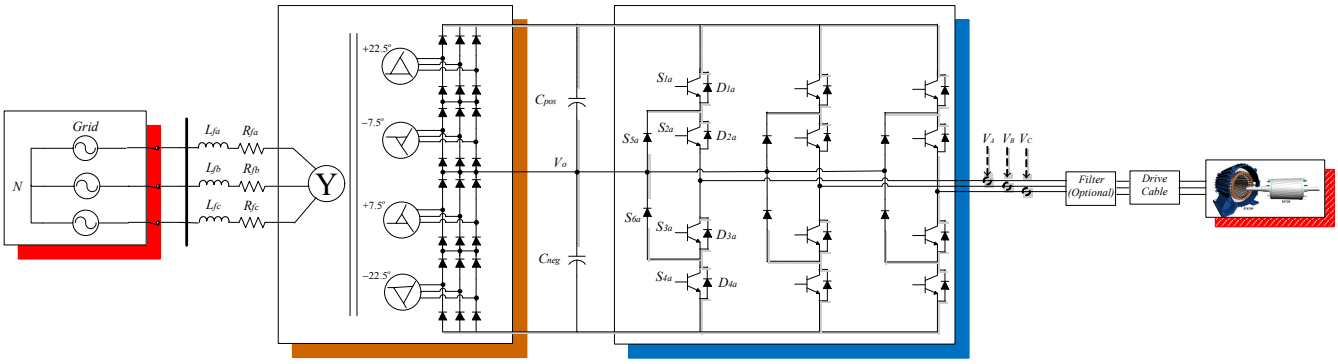

Fig .1. 3L NPC IM MVD System

A three phase dual active bridge (DAB) rectifier is proposed as a replacement of the classic multi-pulse rectifier based on phase-shifting transformers, which is categorized as an isolated three phase PFC rectifier [6]. The common DC link structure is unchanged, which makes it suitable for both single and multiple inverter configurations. In addition to exceeding the performance requirements for the commercial MVD products, it has some unprecedented features inherited in which promote MVDs to high voltage direct current (HVDC) and intelligent energy management (IEM) markets. A three phase DAB rectifier realizes both zero voltage switching (ZVS) and unity PF functions in regardless of the motor loading conditions. Besides, this DAB rectifier is capable of accepting power grid voltage ranged from 2.4 kV to 13.8 kV.

Section II will analyze the proposed 1 MVA three phase DAB rectifier mechanism. First, the circuitry topology and operational strategies are discussed as background knowledge. Second, a high power SiC module, rated at 375 A, 12.5 kV, is investigated and modeled. Third, a dedicated control scheme is developed based on extended-phase-shift (EPS) theory. Section III will focus on system electrical and thermal modeling to demonstrate the system capability, feasibility, operational efficiency and thermal distribution, respectively. Section IV will draw a conclusion and discuss future trends.

II. SYSTEM MODELING AND DESCRIPTION

A. System Configuration

Fig. 2 demonstrates the proposed system architecture. The front-end rectifier circuitry is decoupled from the inverter unit(s) and is considered as the main AC-DC conversion stage interfacing with the grid. Three separate DAB blocks are assigned to each phase of a balanced Y-connected power system. This topology has combined PFC and rectifier functionalities together as a single-stage design.

Each DAB block starts with the diode H-bridge since there is no active front end (AFE) demand. The DC bus sitting on the primary side of the transformer has 120 Hz ripple embedded. A DC-DC converter, which constitutes of six SiC MOSFET switches and the high frequency transformer, regulates the power flow and provides a harmonic-free DC link. The DC link voltage is adjusted to coordinate with the inverter topologies and machine types. One of the inverter control targets is to maximize DC link voltage utilization.

Unlike low voltage (LV) drives, high power (HP) inverters have numerous hardware topologies and modulation techniques which are already commercialized. The inverters can be classified as one of these four families, namely voltage source converter (VSC), current source converter (CSC),

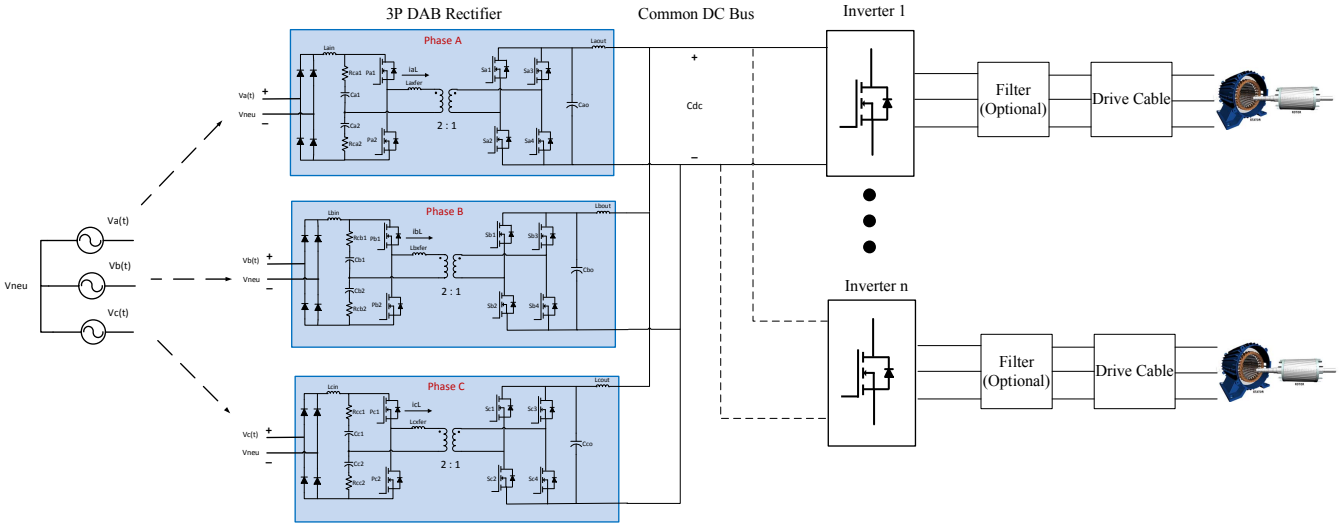

Fig .2. Three Phase DAB Rectifier in MVDs

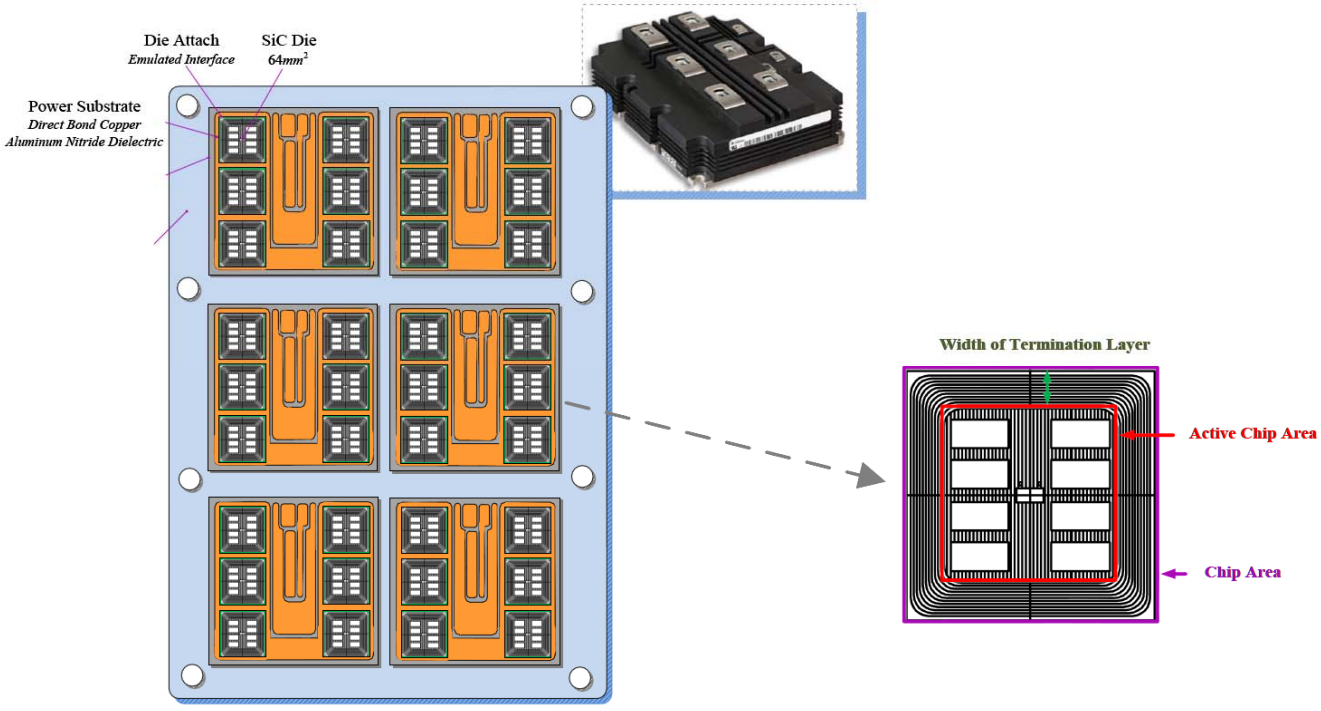

Fig. 3. A Cutaway Drawing of SiC375R12500 (375 A, 12.5 kV) MOSFET Module

cyclonconverter (CCV) and cascaded matrix converter (CMC) [3]. The availability, reliability and cost of the semiconductor devices have a profound impact to the inverter topology selection.

Considering the system integrity, there is a popular discussion in regarding of the configurations between inverter(s) and machine(s). Multiple inverters with backup units are stacked up to provide the power to the machine(s) as a whole package if the system operational redundancy is required. One standard inverter per machine is preferred if each machine is designed and controlled separately. MVDs have the reputation for highly customized and application-oriented design.

B. SiC MOSFET Module (fig. 3)

Silicon (Si) insulated gate bipolar transistors (IGBTs) have dominated the MV VFD market since it is first invented around 1980s. Si IGBTs facilitate the adaption of MV VFD in the modern industrial applications due to some attractive features, like simple gate drive circuit, low conduction loss, mature packaging technology and superior ruggedness. However, Si IGBT is not the ideal candidate for the DAB rectifier because of two reasons. One, the bipolar current conduction mechanism in IGBTs limits the switching speeds, especially in high power modules [7]. Second, the wide band gap semiconductor industry has witnessed rapid growth within last two decades. Some SiC and Gallium Nitride (GaN) products have been successfully released. SiC power devices based on vertical device structure is particularly suitable for high power applications because it can be scaled to higher voltage ratings more easily compared to the lateral GaN power transistors. SiC material has about ten times the electric field strength than Si as well as much higher thermal conductivity. Fig. 4 shows a graphic comparison between SiC, GaN and Si materials in terms of energy gap, melting point, saturation drift velocity, thermal conductivity and breakdown field.

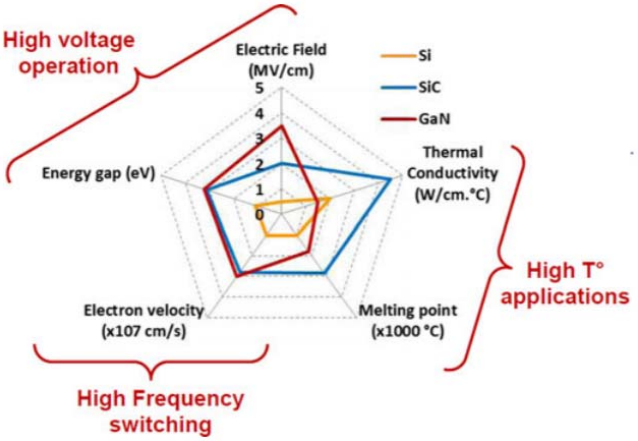

Fig . 4. Summary of Si, SiC and GaN Relevant Material Properties [8].

Prototype 15 kV, 10 A SiC MOSFET samples have been developed by Wolfspeed and tested by the authors' group previously [9]. Starting with the prototype chip, some analyses and derivation are used to estimate the hypothetical SiC MOSFET chip parameters. The modified SiC chip is a cost out version, rated at 10.5 A and 12.5 kV, remains the same size as prototypes. The physical size and chip layout are presented in fig. 5.

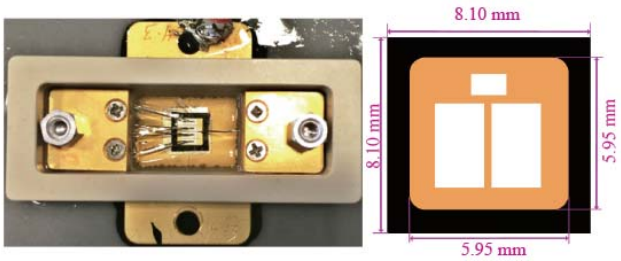

Fig. 5. 15 kV SiC MOSFET, Packaged Module & Die Dimension [10]

(Active Chip: 35.40 mm^2, Chip size 65.61 mm^2)

A hypothetic module includes thirty-six SiC chips, which are connected in parallel. Therefore, the SiC MOSFET module is rated at 12.5 kV, 375 A.

Typically, separate SiC junction barrier schottky (JBS) diodes are added for a practical reason. The MOSFET body diode has the undesirable reverse recovery performance when the massive carriers are implanted by the PN junction. Besides, the device performance degradation and lifetime reduction occurs because of the forward conduction of the PN junction. The additional JBS diodes avoids the body diode conduction on the hardware level [10].

Some research teams have reported this degradation issue been resolved in 1200 V SiC MOSFETs. Assume this similar technology would be applied to this 12.5 kV module, the bode diode can at least conducts for a short period of time without the performance degradation. The strategy is to operate the SiC MOSEET as a synchronous rectifier and conducts current bi-directionally. The body diode only works during the dead time period which is several microsecond per switching event. Therefore, the conduction loss is mitigated due to the low voltage drop across the MOSFET chip. The whole power module is designed more cost-effectively since there is no need to add additional JBS diodes.

Fig. 5 is a cutaway drawing of a SiC 375R12500 (12.5 kV, 375 A) MOSEFT module. The location of SiC die, die attach, power substrate, substrate attach and based plate are highlighted for manufacturing reference. Same power modules are used in both primary and second sides of the DAB rectifier (Fig. 2) for consistency purpose. In order to reduce the module footprint, only single MOSFET module is packaged per case. The plastic case of Infineon FZ750R65KE3 (6.5 kV, 750 A) is selected to standardize the packaging procedure.

Authors laid the groundwork of electrical and thermal modeling of a hypothetic SiC MOSFET module in a previous publication [4]. Based on the test results of a 15 kV, 10 A SiC MOSFET sample [9] and the datasheet of Infineon FZ750R65KE3 Si IGBT module, the parameters and characteristics of a SiC 375R12500 (12.5 kV, 375 A) MOSEFT module are derived.

(1) The relationship between the chip area and the thermal impedance from junction to heat sink is required to demonstrate the power modules' thermal properties.

$$R_{th,JS(SiCMOSFET)} = R_{th,JS(SiIGBT)} \times \frac{A_{chip(Si)} \times N_{Si}}{A_{chip(SiC)} \times N_{SiC}} \approx 38.86\ (K/kW) \quad (1)$$

(2) The SiC MOSFET module conduction loss depends on the load current and drain to source resistor which is temperature dependent. Table I stores the on resistance values under different temperature settings.

Table I Drain to Source Resistance of SiC375R12500 SiC MOSFET Module

$Temperature\ (^oC)$	$R_{DS(on)}\ (m\Omega)$, $V_{GS} = 20\ (V)$
25	10.6
75	16.4
125	26.0
175	41.5
225	59.8

$$P_{Cond,MOSFET}(I) = R_{DS(on)} \times I^2 \quad (2)$$

(3) Theoretically, there is no switching losses because of ZVS implementation. For integrity purpose, the switching loss model is stated for future reference.

The energy per switching event is associated with chip area, transient current, voltage drop between collector and emitter. The switching frequency is involved in the switching loss calculation. (3) and (4) are numerical equations for the module switching losses.

$$\begin{cases} E_{on}(I) = N_{chip} \times E_{on}(0A) \times \sqrt{\dfrac{15}{12.5}} + 0.5 \times I\ (mJ) \\ \qquad\qquad \approx 36 \times 4.5 \times 1.10 + 0.5 \times I\ (mJ) \\ E_{off}(I) \approx 0\ (mJ) \end{cases} \quad (3)$$

$$P_{Swiching} = f_s \times [E_{on}(A_{chip}, I_{ds}, U_{ds}) + E_{off}(A_{chip}, I_{ds}, U_{ds})] \quad (4)$$

C. DAB Control Scheme

The DAB isolated converter has become a standard option in the AC-DC power conversion system, which serves as a core part in the electricity infrastructure when a output DC link is demanded. Compared with transformer-less topologies, the DAB circuit provides a galvanic isolation which improves the system's tolerance under catastrophic failures. The DAB converter has been researched and targeted to some LV applications, like electric vehicles, storage batteries for the uninterruptible power supplies (UPS) or energy interface of photovoltaic (PV) panels. If the SiC module proposed in fig. 5 could be prototyped, DAB rectifier will have a significant impact to the MVDs which is currently dominated by Si IGBT technology.

The conventional AC-DC isolated rectifier consists of a power factor rectifier and a subsequent high-frequency (HF)

DC-DC converter. A review of single-stage isolated ac-dc PFC converters and single-phase non-isolated PFCs has been given in [11] [12]. The proposed three phase DAB rectifier has three individual single-stage isolated ac-dc converters which regulate the same DC link and share the load.

The control strategies are developed and optimized based on the pre-defined or predictive operational conditions. Key control objectives are summarized as below,

(i) Conservation of energy must be secured for safe operation requirements.

(ii) PFC feature is favored to eliminate the reactive power consumption.

(iii) ZVS of all active devices is suggested to elevate the system efficiency. Furthermore, only ZVS turn-on is one of the control targets because the turn-off losses are negligible per (3).

(iv) The reactive power mitigation and the HF transformer leakage current decrease are two optimization goals.

(v) The system is immune to the voltage ripple and accepts wide range of the grid voltage, given 2.4 kV to 13.8 kV.

(vi) The control scheme has self-tuned capability to guarantee all above features in regardless of motor loading conditions.

Four major control methods, like single phase shift (SPS), extended phase shift (EPS), dual phase shift (DPS) and triple phase shift (TPS), are reported in [4]. The control methodology proposed in this paper is a mixture of SPS and EPS. Three control variables are listed as below,

(a) The device switching frequency is defined as f_s.

(b) D_1 is the phase shift between primary side half bridge and secondary side full bridge circuits.

(c) D_2 presents the phase shift between two legs of the full bridge sitting on the secondary side of the HF transformer.

The control strategy is to stay with SPS if applicable because the wider effective pulse of SPS decreases the transformer leakage RMS current. The EPS mode is enabled only if SPS reaches its limits. the SPS2 is developed to resolve the current distortion issue when the input grid voltage has relatively low instantaneous value or the electrical machine is either unloaded or lightly loaded [13]. Three modes are named as SPS1, EPS, SPS2 covering all the operational conditions. Differ to the traditional SPS algorithm, the center controller uses the system variables as the guideline to determine when and how to activate each algorithm respectively. The intensive calculation workload can be done off-line and the results are stored as look up tables to increase the controller response time.

III. SYSTEM MODELING AND DESCRIPTION

A time-domain simulation platform has Piecewise Linear Electrical Circuit Simulation (PLECS) for circuitry thermal model been co-simulated with control algorithm implemented in MATLAB/Simulink environment. A case study based on an industrial MVD project is referred as the proof of concept project. Table II itemizes the parameters of a bench mark system.

Table II System Parameters of a Three-phase DAB Rectifier

Input and Output Ratings		
Power rating	S_{rating}	1 MVA
Grid voltage (RMS)	V_{grid}	12.5 kV
Line frequency	f_{grid}	60 Hz
DC link voltage	V_{dc}	6 kV
Motor terminal voltage	V_{motor}	4.16 kV
Semiconductor (SiC MOSFETs) Ratings		
Voltage rating	V_{mosfet}	12.5 kV
Current rating	I_{mosfet}	375 A
Switching frequency	f_{mosfet}	< = 50 kHz
High Frequency Transformer		
Leakage inductance	L_{xfer}	6.5 mH
Turns Ratio	$n:1$	2:1

A. *Input and Output Waveforms*

Fig. 6 and fig. 7 show the power grid voltage and current. The unity power factor is guaranteed in regardless of the phase angle. The EPS technique delicately smooths the current when a voltage zero-crossing occurs. Hence, the current THD gets improved to 6.98% which is a selling point of grid-tied converter products.

Fig. 8 shows the output DC link voltage, current and power, which are free of harmonics. Thus, the DC link serves as a clean power supply to the inverter circuits. The output power is measured approximately 1 MVA and keeps constant over a line cycle.

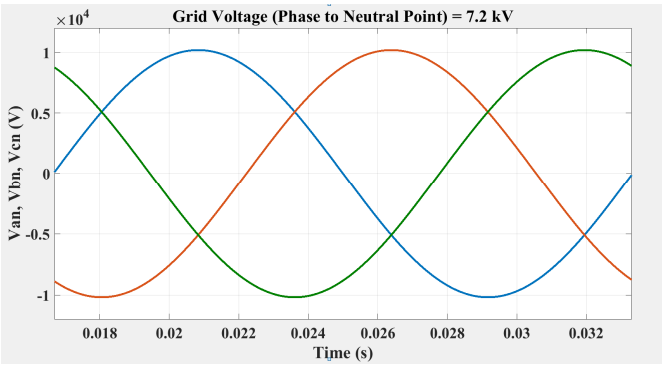

Fig. 6. Three Phase Grid Voltages

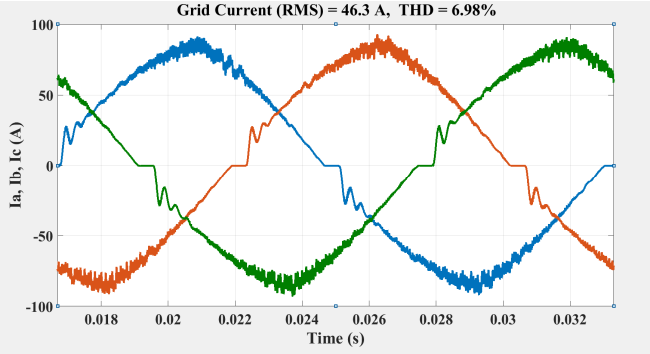

Fig. 7. Three Phase Grid Currents

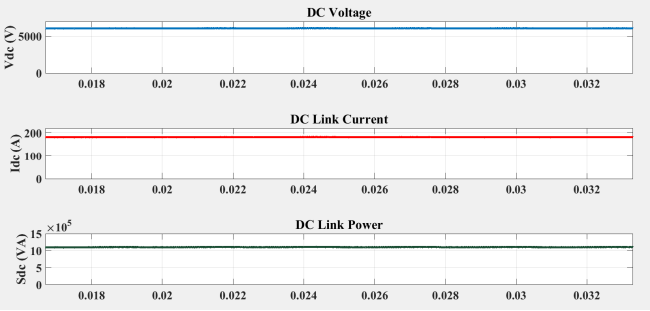

Fig. 8. DC Link Voltage, Current, Power

B. Transformer and Semiconductor Waveforms

Fig. 9 - fig. 11 present two voltages and one current of the transformer. The primary, secondary winding voltages and the leakage current are selected to demonstrate the system behaviors in either SPS or EPS mode.

Fig. 12 and fig. 13 present the voltage and current of two MOSFETs; i.e. P1 (primary side device) and S1 (secondary side device). ZVS turn-on checking points are highlighted in purple and achieved under both SPS and EPS operational circumstances.

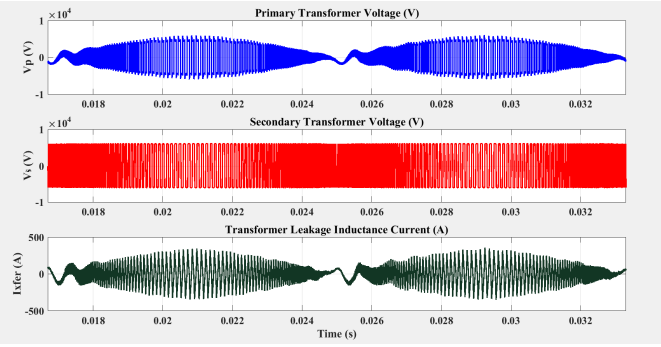

Fig. 9. Transformer Voltage & Current

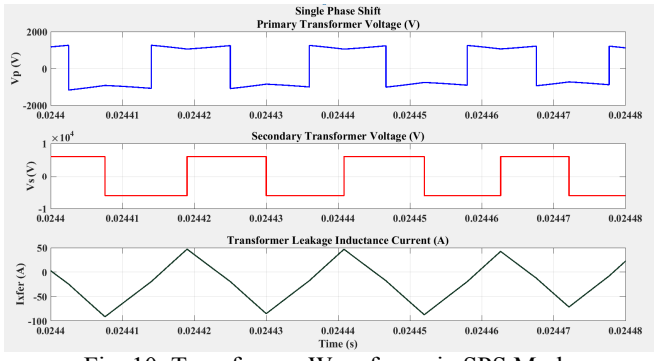

Fig. 10. Transformer Waveforms in SPS Mode

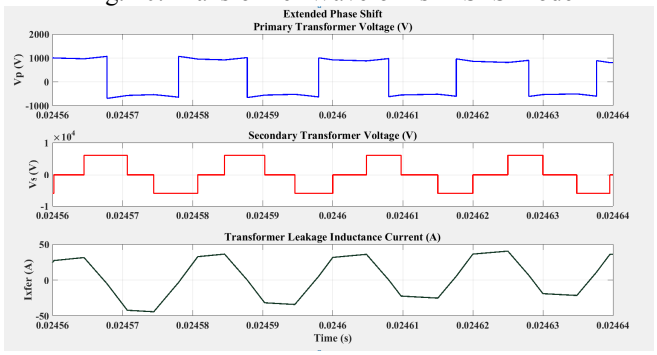

Fig. 11. Transformer Waveforms in EPS Mode

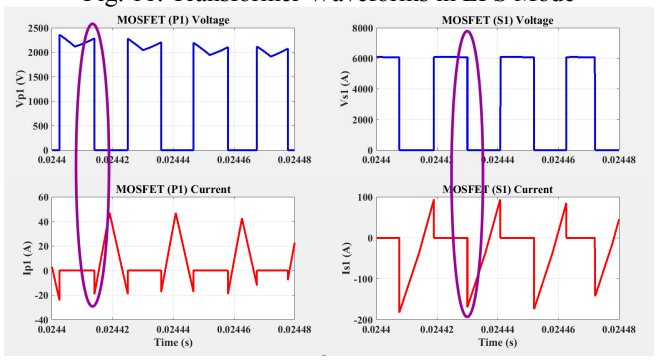

Fig. 12. ZVS Turn on Checking of Primary Side MOSFET (P1) and Secondary Side MOSFET (S1) in SPS Mode

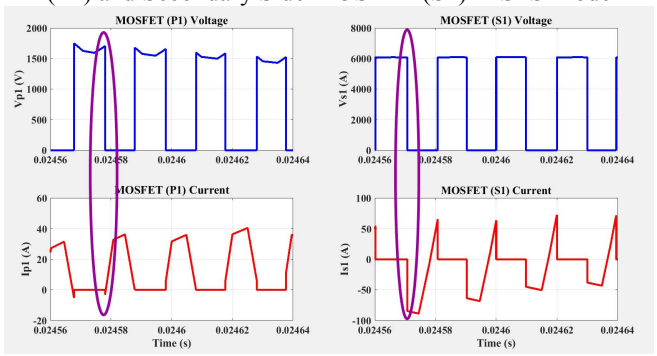

Fig. 13. ZVS Turn on Checking of Primary Side MOSFET (P1) and Secondary Side MOSFET (S1) in EPS Mode

C. Power Loss Model

The power loss and thermal models of SiC 375R12500 (12.5 kV, 375A) MOSFET are developed in PLECS. Equations (1)

to (4) and table I provide the mathematic expressions in related to the thermal impedance from junction to heat sink $R_{th,JS}$, conduction loss $P_{Cond,MOSFET}(I)$, turn on $E_{on}(I)$ and turn off $E_{off}(I)$ energy and switching loss switching loss $P_{switching}$.

Table III illustrates the power loss distribution of a 1 MVA SiC DAB rectifier. The system is 100 % loaded with rated grid voltage.

TABLE III 1 MVA SiC MV Three Phase DAB Rectifier Power Loss Distribution

Location	Designator	Conduction Loss (W)	Switching Loss (W)
Transformer Primary Side	P1	305	0
	P2	307	0
Transformer Secondary Side	S1	420	0
	S2	426	0
	S3	442	0
	S4	427	0
3 Phase DAB Rectifier		6981	0
System Efficiency		99.3%	

D. Advanced Feature I – Ultra-wide Range of Grid Voltage

Three phase DAB rectifier is capable of accepting ultra-wide range of grid voltage. The hardware design specification is scoped by considering varying grid voltage levels. The main controller is robust enough to keep the DC link voltage stabilized at 6 kV by manipulating the semiconductor gating signals. Fig. 14 to fig. 16 are the graphic diagrams of operating time of SPS and EPS when the phase voltage varies from 1 kV to 8 kV. Per discussed in section II topic C, a special SPS (SPS2) is triggered at either low grid input voltage or light load situation.

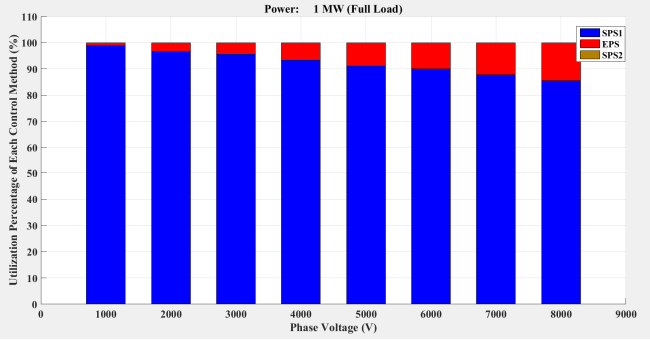

Fig. 14 Utilization Percentage of SPS and EPS When Phase Voltage Varies from 1 kV to 8 kV. Machine is 100 % loaded.

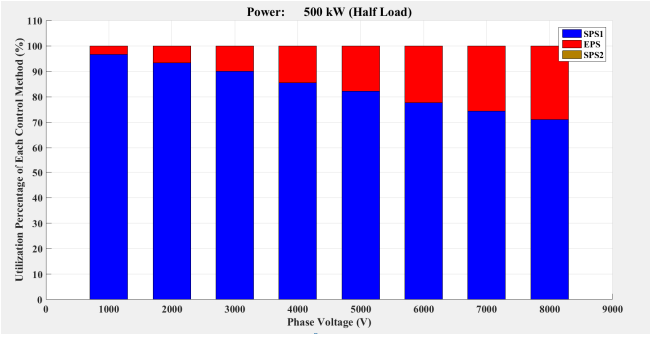

Fig. 15 Utilization Percentage of SPS and EPS When Phase Voltage Varies from 1 kV to 8 kV. Machine is 50 % loaded.

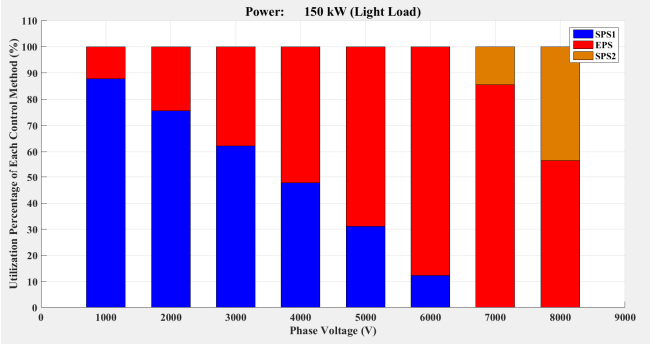

Fig. 16 Utilization Percentage of SPS and EPS When Phase Voltage Varies from 1 kV to 8 kV. Machine is 15 % loaded.

E. Advanced Feature II – Custom Motor Load Profiles.

Per discussed in section I, the traditional phase-shifting transformer rectifier has worse current THD and power factor if the motor is partially loaded. In contrast, three phase DAB rectifier is not sensitive to the load profiles. Similar to the last topic, the controller actively monitors the power flow and uses it as a input variable in calculating the device firing angles. Fig. 17 to fig. 19 are the graphic diagrams of operating time of SPS and EPS when the motor is loaded from 5 % to 115 % with 5% increment.

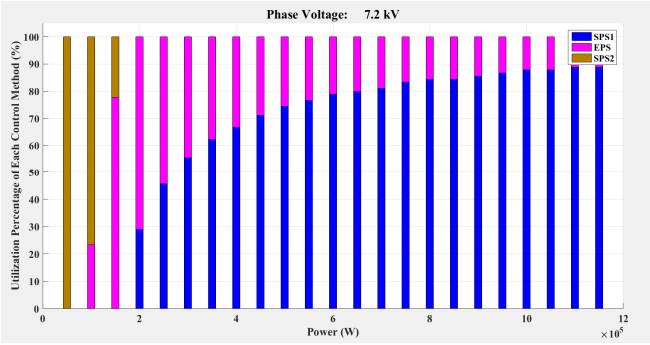

Fig. 17 Utilization Percentage of SPS and EPS under Different Loads. Phase Voltage is 7.2 kV.

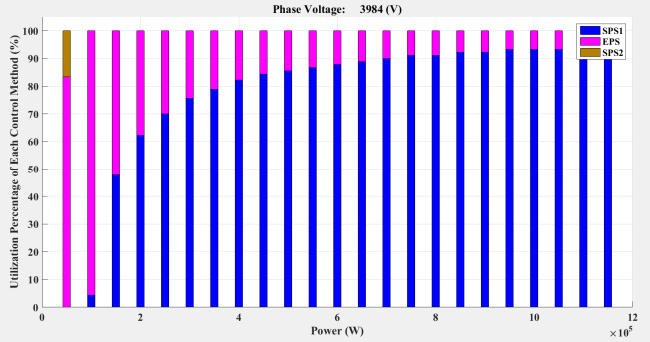

Fig. 18 Utilization Percentage of SPS and EPS under Different Loads. Phase Voltage is 4 kV.

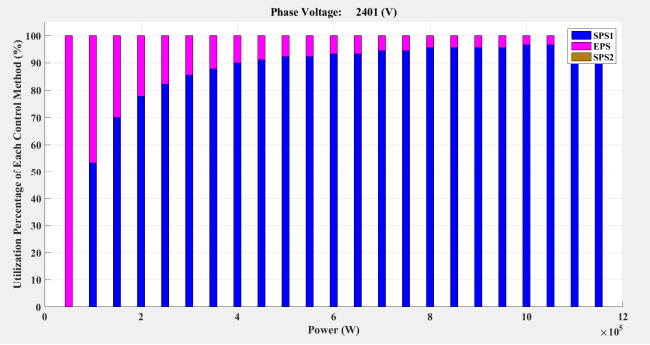

Fig. 19 Utilization Percentage of SPS and EPS under Different Loads. Phase Voltage is 2.4 kV.

IV. CONCLUSIONS

The paper has investigated the performance of a 1 MVA SiC MV three phase rectifier based on isolated DAB topology. Compared with the traditional multi-pulse rectifier based on phase-shifting transformers, the proposed circuit meets all the performance requirements with higher power density and operational efficiency. Two advanced features brought by DAB rectifier never were offered by commercial MVD products. One is the ultra-wide range of grid voltage input. Another one is the custom motor load profiles. Both of these provide the operational and economic feasibilities and elevate the system performance to the next level.

A hypothetic SiC MOSFET is proposed rated at 12.5 kV and 375 A. The internal chip layout is covered. Both electrical and thermal characteristics are analyzed and mathematically modeled.

A hybrid control scheme involving both SPS and EPS algorithms ensures the DAB rectifier has superior performances in both steady state and transient time.

A simulation environment including Matlab/Simulink and PLECS blockset has been established. All mentioned concepts have been fully proven in section III.

There is no doubt some design work is required to manufacture a DAB rectifier, such as gate driver development, EMI/EMC noise immunity enforcement, etc. Furthermore, the control algorithm, like ZVS feature, can be optimized based on the characteristics of core components.

REFERENCES

[1] H. Abu-Rub, J. Holtz, J. Rodriguez and G. Baoming, "Medium-Voltage Multilevel Converters—State of the Art, Challenges, and Requirements in Industrial Applications," in *IEEE Transactions on Industrial Electronics*, vol. 57, no. 8, pp. 2581-2596, Aug. 2010.

[2] F. Zare; P. Davari; F. Blaabjerg, "A Modular Active Front-End Rectifier with Electronic Phase-Shifting for Harmonic Mitigation in Motor Drive Applications," in *IEEE Transactions on Industry Applications* , vol.PP, no.99, pp.1-1, July. 2017.

[3] H. Tang and A. Q. Huang, "Assessment of medium voltage SiC MOSFET advantages in medium voltage drive application," *2017 IEEE Energy Conversion Congress and Exposition (ECCE)*, Cincinnati, OH, USA, 2017, pp. 801-807.

[4] S. Kouro, J. Rodriguez, B. Wu, S. Bernet and M. Perez, "Powering the Future of Industry: High-Power Adjustable Speed Drive Topologies," in *IEEE Industry Applications Magazine*, vol. 18, no. 4, pp. 26-39, July-Aug.

[5] D. Kumar and F. Zare, "Harmonic Analysis of Grid Connected Power Electronic Systems in Low Voltage Distribution Networks," in *IEEE Journal of Emerging and Selected Topics in Power Electronics*, vol. 4, no. 1, pp. 70-79, March 2016.

[6] B. Zhao, Q. Song, W. Liu and Y. Sun, "Overview of Dual-Active-Bridge Isolated Bidirectional DC–DC Converter for High-Frequency-Link Power-Conversion System," in *IEEE Transactions on Power Electronics*, vol. 29, no. 8, pp. 4091-4106, Aug. 2014.

[7] X. She, A. Q. Huang, Ó. Lucía and B. Ozpineci, "Review of Silicon Carbide Power Devices and Their Applications," in *IEEE Transactions on Industrial Electronics*, vol. 64, no. 10, pp. 8193-8205, Oct. 2017.

[8] J. Millán, P. Godignon, X. Perpiñà, A. Pérez-Tomás and J. Rebollo, "A Survey of Wide Bandgap Power Semiconductor Devices," in *IEEE Transactions on Power Electronics*, vol. 29, no. 5, pp. 2155-2163, May 2014.

[9] G. Wang, A. Q. Huang *et al*., "Static and dynamic performance characterization and comparison of 15 kV SiC MOSFET and 15 kV SiC n-IGBTs," *2015 IEEE 27th International Symposium on Power Semiconductor Devices & IC's (ISPSD)*, Hong Kong, 2015, pp. 229-232.

[10] A. Q. Huang, Q. Zhu, L. Wang and L. Zhang, "15 kV SiC MOSFET: An enabling technology for medium voltage solid state transformers," in *CPSS Transactions on Power Electronics and Applications*, vol. 2, no. 2, pp. 118-130, 2017.

[11] B. Singh, B. N. Singh, A. Chandra, K. Al-Haddad, A. Pandey and D. P. Kothari, "A review of single-phase improved power quality AC-DC converters," in *IEEE Transactions on Industrial Electronics*, vol. 50, no. 5, pp. 962-981, Oct. 2003.

[12] J. P. M. Figueiredo, F. L. Tofoli and B. L. A. Silva, "A review of single-phase PFC topologies based on the boost converter," *2010 9th IEEE/IAS International Conference on Industry Applications - INDUSCON 2010*, Sao Paulo, 2010, pp. 1-6.

[13] Tian *et al*., "A novel light load performance enhanced variable-switching-frequency and hybrid single-dual-phase-shift control for single-stage dual-active-bridge based AC/DC converter," *IECON 2016 - 42nd Annual Conference of the IEEE Industrial Electronics Society*, Florence, 2016, pp. 1227-1232.